

## **EFFECTIVE ADSORPTIVE REMOVAL OF PENTACHLOROPHENOL IN WATER USING MAGNETICAL MANGANESE FERRITE NANOPARTICLES IMMOBILIZED ON DOMESTIC ACTIVATED CARBON**

LE BAO HUNG <sup>(1,3)</sup>, NGHIEM XUAN TRUONG <sup>(1)</sup>, NGUYEN THI THU HANG <sup>(1)</sup>, VU MINH CHAU <sup>(1)</sup>, NGUYEN DUC THANG <sup>(1)</sup>, NGUYEN THI NANG <sup>(1)</sup>, DANG MINH QUANG <sup>(1)</sup>, CAO PHUONG ANH <sup>(1)</sup>, DAO NGOC NHIEM <sup>(2,3)</sup>, NGUYEN TRUNG KIEN <sup>(2)</sup>

### **1. GENERAL INTRODUCTION**

Chlorinated phenol (CP) compounds are persistent organic pollutants that have been widely used in various industrial applications, including pesticide production, pharmaceuticals, textiles, refineries [1, 2]. However, even a small amount of these compounds in industrial wastewater can cause significant environmental damage, particularly to aquatic ecosystems, and pose serious health risks to living organisms, including liver, kidney, blood, and nervous systems disorders [2]. To face the challenge of CP remediation in water, numerous useful techniques have been developed and exhibited their effectiveness, for example, electrochemical oxidation, photodegradation, membrane separation, and adsorption. Amongst, due to its simplicity, high efficiency, and low cost, adsorption has been widely used in numerous wastewater treatment plants (WWTPs).

A variety of adsorbents, such as activated carbons (ACs), zeolites, or kaolinites, have been studied for the adsorptive removal of CPs [3-5]. ACs, which can be produced from different sources, have exhibited outstanding characteristics for the adsorptive removal of contaminants in water. Because of its high specific area and porosity, simple preparation, excellent treatment efficiency, environmental friendliness, and low cost, ACs play a crucial role in many WWTPs that employ adsorption. However, the separation of ACs from WWTPs after treatment also poses many problems, especially with the use at micro- to nano-scales.

To handle this issue, the ideas about magnetized ACs (MACs) as effective adsorbents have been developed and have resulted in many promising outcomes. By applying an external magnetic field, the used MACs can be quickly recovered from the aqueous solution. The magnetized ACs were commonly prepared by fabrication with  $\text{Fe}_3\text{O}_4$  or ferrite ( $\text{MFe}_2\text{O}_4$ ) nanoparticles (NPs) [6-8]. In this study, the surface of AC adsorbent has been modified with the immobilization of manganese ferrite  $\text{MnFe}_2\text{O}_4$  (MFO) NPs using a simple gel-combustion method. The obtained (MFC) samples were thoroughly characterized before examining the capability of adsorptive removal of pentachlorophenol (PCP), a highly toxic chlorinated phenol, from aqueous solutions.

## 2. EXPERIMENTAL

### 2.1. Chemicals

$\text{Fe}(\text{NO}_3)_3 \cdot 9\text{H}_2\text{O}$ ,  $\text{Mn}(\text{NO}_3)_2 \cdot 4\text{H}_2\text{O}$ ,  $\text{HCl}$ , and  $\text{NaOH}$  were purchased from Aladdin Industrial Corporation (China). AC was domestically provided by Tra Bac Joint Stock Company (Vietnam) (Table 1). Polyvinyl alcohol (PVA,  $M = 145,000 \text{ g} \cdot \text{mol}^{-1}$ ), methanol ( $\text{MeOH}$ ), and acetonitrile ( $\text{ACN}$ ) were purchased from Sigma-Aldrich. PCP was supplied by AccuStandard (USA). All reagents were used as received from the provider without further purification.

**Table 1.** General details of used AC for this study

Iodine content	1.041 $\text{mg} \cdot \text{g}^{-1}$
Moisture	2.80%
Bulk density	506 $\text{g} \cdot \text{L}^{-1}$
pH	6.60
Grain size	0.425 - 0.85 mm (98.40%)

### 2.2. Materials preparation and characterization

MFO and MFC were prepared following our previous study [9] with the precursor  $\text{Fe}(\text{NO}_3)_3 \cdot 9\text{H}_2\text{O}$ ,  $\text{Mn}(\text{NO}_3)_2 \cdot 4\text{H}_2\text{O}$ , and AC ( $\text{Fe}^{3+}/\text{Mn}^{2+}$  atomic ratio = 9:1, AC/MFO w/w = 0.10:1). The obtained MFC and MFC were firstly characterized by X-ray diffraction (XRD) using a  $\text{Cu K}\alpha$  radiation of a D8 Advance X-ray diffractometer (Germany) and a S-4800 scanning electron microscope (SEM) by Hitachi (Japan). An Energy-dispersive X-ray spectroscopy (EDX) coupled with SEM apparatus was also used for the determination of elemental composition. Fourier-transform infrared (FTIR) spectra of synthesized materials were recorded at room temperature using a Shimadzu FTIR spectrometer (Japan) in the 400 - 4000  $\text{cm}^{-1}$  range. Nitrogen adsorption isotherms were performed at  $-196 \text{ }^\circ\text{C}$  on an Autosorb IQ Station in order to calculate the specific surface area ( $S_{\text{BET}}$ ) of obtained materials. The magnetic properties of the prepared materials were investigated using a vibrating sample magnetometer (VSM) with a sensitivity of  $10^{-4}$  emu, applied magnetic fields range of -10 to 10 kOe at the temperature range of 77 - 1000 K. The zeta potentials of MFC were measured at  $25 \text{ }^\circ\text{C}$  using a zeta potential analyzer (Malvern Instruments Ltd, England).

### 2.3. PCP adsorption experiments

For the adsorption experiments, 250-mL-Erlenmeyer flasks equipped with a mechanical stirrer were employed. First, 30 mg of AC, MFO, and MFC was added to 100 mL of PCP 25 ppm solutions. The flasks were shaken for 24 hours at ambient temperature to certainly approach the equilibrium. For the investigation of absorption conditions, MFC was used. While pH values ranged from 3 to 10, adjusted using  $\text{HCl}$  and  $\text{NaOH}$  solution. The adsorbent contents and initial PCP

concentration were varied from 100 to 1000 mg/L and 10 to 60 mg/L, respectively. After a certain time, 1 mL of the solution was taken from the solution, filtered, and evaluated by a liquid chromatography triple quadrupole system (LC/MS/MS) to determine the PCP concentration. The LC/MS/MS system was operated with the conditions recorded in our previous study [9]. The following equation determines the adsorption efficiency of PCP at time  $t$  (Eq. 1):

$$H(\%) = \frac{C_0 - C_t}{C_0} \times 100\% = \frac{A_0 - A_t}{A_0} \times 100\% \quad (1)$$

where  $A_0$  and  $A_t$  are the peak area of PCP ( $m/z = 265.5$ ) at 0 and  $t$  hours obtained from the LC/MS/MS system, and  $C_0$  and  $C_t$  are the concentration of PCP at 0 and  $t$  min, respectively.

### 3. RESULTS AND DISCUSSION

#### 3.1. Materials characterization

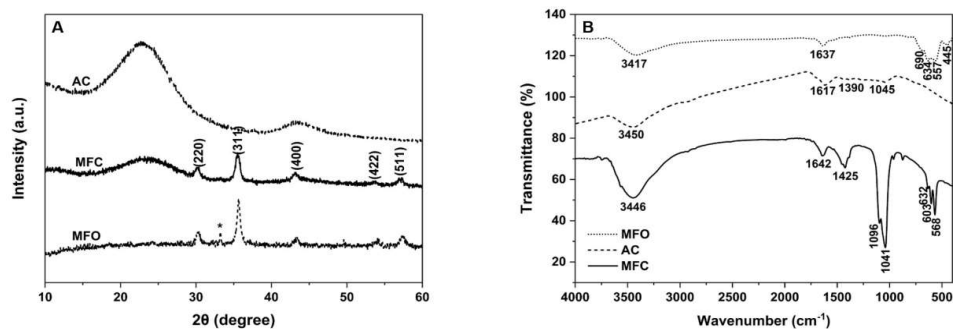


**Figure 1.** (A) XRD and (B) FTIR curves of prepared MFC and MFO samples

Firstly, the crystalline phase of MFC was evaluated by an XRD analysis (Fig. 1A). The main diffraction peaks were recorded at  $2\theta$  values of  $30.20^\circ$ ,  $35.53^\circ$ ,  $43.94^\circ$ ,  $53.68^\circ$ , and  $57.11^\circ$ , which were attributed to the (220), (311), (400), (422), and (511) planes of a face-centered cubic structure of spinel MFO nanoparticles (JCPDS Card No. 073-1964). In addition, a broadened peak centered at  $23.1^\circ$  represented a characteristic diffraction of the AC sample. Moreover, a peak marked by an asterisk (\*) in the MFO curve, assigned to the  $\alpha$ - $\text{Fe}_2\text{O}_3$  phase, mostly disappeared in the MFC curve. No other unusual peaks were observed for the MFC sample. According to the Debye-Scherrer equation [9], the calculated crystal size of MFO NPs on the MFC sample corresponding to the diffraction of the (311) plane was 11.63 nm.

Secondly, functional groups that existed in the MFC sample were examined (Fig. 1B). All examined materials display characteristic peaks of the stretching O-H bonds of absorbed water molecules at approximately  $3400$  and  $1640 \text{ cm}^{-1}$ . Other adsorption peaks in the range of  $900 - 1700 \text{ cm}^{-1}$  were attributed to linkages of C-C as well as C-O of absorbed atmospheric  $\text{CO}_2$ , AC, and PVA residues. On the other hand, the vibration of metal-oxygen bonds in the tetrahedral structure located in the range of  $500 - 700 \text{ cm}^{-1}$  were observed for both MFO and MFC curves, but not in the AC curve.

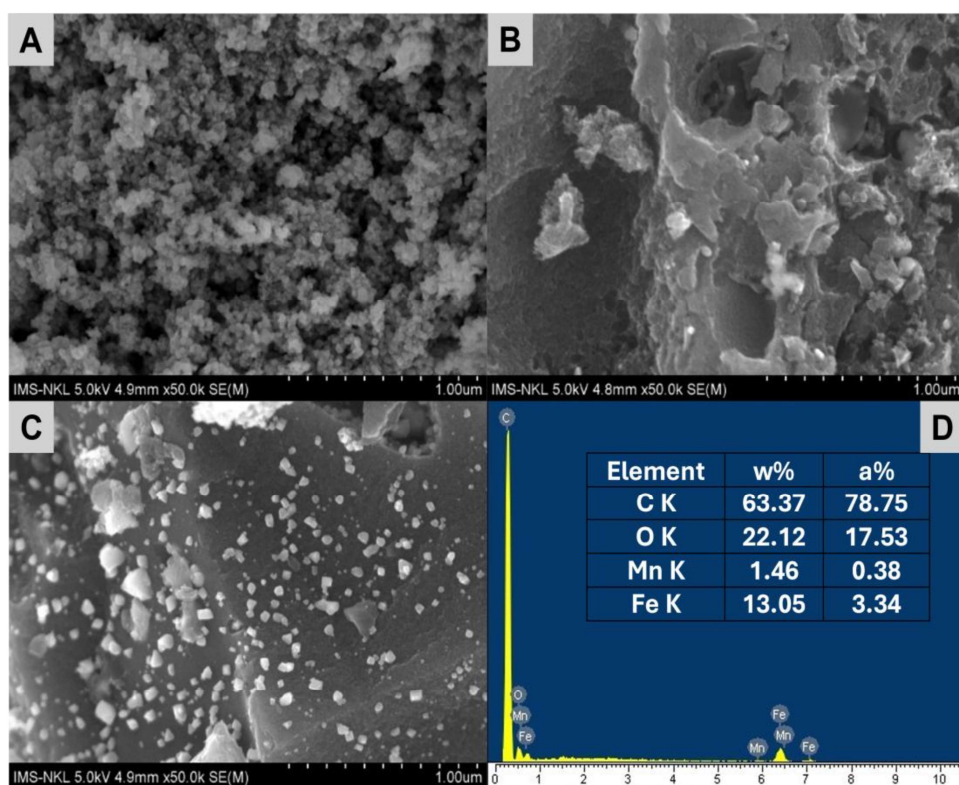


**Figure 2.** SEM images of (A) MFO, (B) AC, and (C) MFC. (D) Elemental analysis and EDX spectra of MFC

The SEM images of MFO, AC, and MFC samples are presented in Fig. 2A - 2C. It can be easily observed the dispersion of cubic-like MFO NPs onto the surface of AC material. The elemental analysis by EDX confirmed the presence of C, O, Mn, and Fe in the MFC sample (Fig. 2D). Carbon (78.75%), mainly from AC, was the major element in MFC, while the atomic percentage of Fe and Mn were 3.34% and 0.38%, respectively, which was consistent with the  $\text{Fe}^{3+}/\text{Mn}^{2+}$  molar ratio (9:1 a/a) in the precursors. The results of morphology, elemental, and functional group analyses suggest that MFC samples were successfully prepared in this study.

To evaluate the magnetic properties of the modified AC sample, VSM measurements were performed on bare AC, MFO, and MFC samples (Fig. 3A). While the bare AC sample hardly exhibited the magnetic properties, both MFO and MFC demonstrated their paramagnetic characteristics in the applied magnetic field. The saturation magnetization of MFO and MFC samples has values of 34.10 and 15.98 emu/g, respectively. This result suggests that the surface of AC samples was successfully magnetized with a significant amount of magnetic MFO NPs.

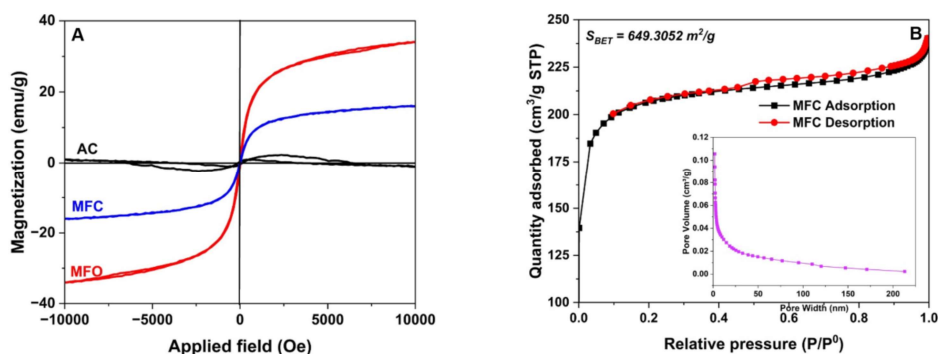


**Figure 3.** (A) VSM and (B) N<sub>2</sub> adsorption isotherm of MFC sample.

Finally, the N<sub>2</sub> adsorption isotherm of MFC was conducted, and the results are illustrated in Fig. 3B. MFC shows the type IV nitrogen adsorption-desorption isotherms with H4 hysteresis loops, which are commonly attributed to the presence of micropores and mesopores with interconnected slit-like micropore arrays. The hysteresis loops of MFC began at a relative pressure of about 0.45. From this measurement, the calculated BET specific surface area ( $S_{BET}$ ), pore volume, and pore size of MFC materials are 649.3 m<sup>2</sup>/g, 0.1057 cm<sup>3</sup>/g, and 3.5 - 5.8 nm, respectively.

### 3.2. Evaluation on adsorptive removals of PCP using prepared MFC adsorbent

Initially, the PCP adsorption efficiency (ADE) of MFC was evaluated in comparison with bare AC and MFO samples (Fig. 4A). For all materials, the adsorption quickly occurred in the first 12 hours before slowing down and getting an equilibrium state at about 24 hours. Both MFC and AC samples demonstrated a remarkably higher PCP ADE (90.13% and 92.97%, respectively) compared to MFO NPs (73.60%) after 24 hours of adsorption. Especially under the evaluated adsorption conditions, the magnetized AC sample exhibited analogous PCP adsorbability to the unmodified one, suggesting that the fabrication process does not alter the adsorptive nature of AC and may even enhance its effectiveness of removing PCP.

To elucidate the PCP adsorption on MFC materials that the effects of several experimental conditions, including pH, adsorbent dosage, and initial PCP concentration, were examined. Fig. 4B shows the effect of pH on PCP adsorption on MFC materials. Since the pH values affect the ionic form of both PCP and the surface MFC adsorbent, it would play a crucial role in PCP adsorption. The adsorption at a slightly acidic solution (pH 5) demonstrated the highest ADE (96.32%) and significantly decreased at the more acidic or alkaline media. To explain, the measurement for the zeta potential of MFC was conducted in the pH range of 3 - 10 to determine the isoelectric point (IEP), which was found to be of 6.3

(inset of Fig. 4B). At pH 3, while PCP ( $pK_a = 4.2 - 4.9$ ) is hardly deprotonated, MFC sample is positively charged, leading to a poor adsorbability of PCP onto MFC surface. At pH 5, PCP is more likely to deprotonate to form  $PCP^-$ , whereas MFC is still positively charged. Consequently, the adsorption of PCP onto the MFC surface is facilitated. In contrast, in neutral or more alkaline media (pH 7, pH 10 > IEP), the MFC surface gets negatively charged, which lowers the PCP adsorbability. Hence, it is reasonable to conduct the adsorption of PCP on MFC within the pH range of 5.0 - 6.0 for subsequent investigations.

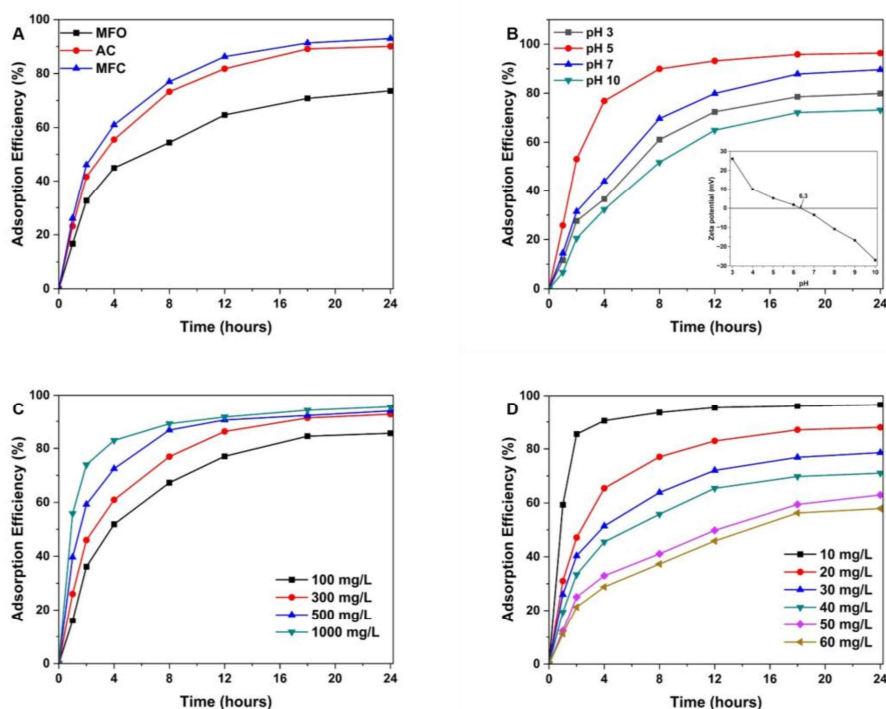


**Figure 4.** Influence of various conditions on PCP adsorption efficiency: (A) used adsorbents, (B) pH (inset: zeta potential of MFC at different pH values), (C) material dosage, and (D) initial PCP concentration

In the following series of experiments, the MFC dosage was varied from 100 to 1000 mg/L (Fig. 4C). Obviously, after 24 hours of adsorption, the PCP ADE demonstrated a proportional tendency with the increase of the adsorbent quantity. In addition, at a higher dosage, the adsorption equilibrium state was reached earlier, within 8 - 12 hours, while the lower ones that state was reached after about 18 - 24 hours. This behavior can be explained that a higher quantity of adsorbent can provide a higher density of adsorptive centers, which facilitates the adsorption of contaminants onto the materials.

Finally, a series of adsorptions with different initial PCP concentrations were carried out (Fig. 4D). An MFC dosage of 300 mg/L with pH 5 of the working solutions was utilized for the examination of concentration influences. Since the initial PCP concentrations increased from 10 mg/L to 60 mg/L, the ADE after 24 hours of adsorption illustrated an inverse change with a drop from 96.53% (PCP 10 mg/L) to 57.89% (60 mg/L). At a low PCP concentration, the equilibrium state was mostly reached at a short adsorption time, about 4 - 8 hours. Meanwhile, at a higher pollutant concentration, it took a long adsorption time of about 18 - 24 hours to reach that state. The reason is that the higher PCP concentration surpassed the adsorption capacity of the used MFC materials. At a low concentration of PCP, the MFC surface and pores can afford the immobilization of PCP molecules and the formation of the linkages between the adsorbent and the contaminants. Meanwhile, further increases in the number of PCP molecules outweighed the quantity of available active adsorptive centers and pores. Consequently, the adsorption is more sluggish with a lower ADE value at the higher PCP concentration.

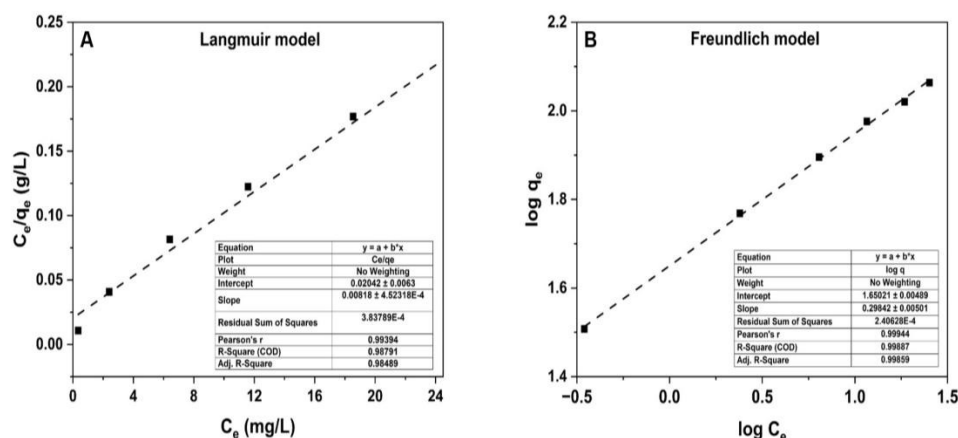


**Figure 5.** Linearized (A) Langmuir and (B) Freundlich models for the PCP adsorption isotherm on MFC adsorbent.

Ultimately, the common Langmuir (Eq. 2) and Freundlich (Eq. 4) models were employed for the assessment of PCP adsorption on MFC samples [10]. The linearized fitting of the Langmuir (linearized form I) (Eq. 3) and Freundlich (Eq. 5) models was described in Fig 5 and as follows:

$$q_e = \frac{q_{max} \cdot K_L \cdot C_e}{1 + K_L \cdot C_e} \quad (2) \leftrightarrow \frac{C_e}{q_e} = \frac{1}{q_{max} \cdot K_L} + \frac{C_e}{q_{max}} \quad (3)$$

$$q_e = K_F C_e^{1/n} \quad (4) \leftrightarrow \log q_e = \log K_F + \frac{1}{n} \log C_e \quad (5)$$

where  $q_e$  is the equilibrium adsorption capacity,  $K_L$  is the Langmuir constant,  $C_e$  is the concentration of PCP at equilibrium,  $q_{max}$  is the maximum adsorption capacity, and  $K_F$  and  $n$  are the Freundlich constants.

Both the linearization of Langmuir and Freundlich models for PCP adsorption on MFC materials demonstrated a similar degree of fitting, with the  $R^2$  values of 0.988 and 0.999, respectively. However, the higher  $R^2$  value with the  $n$  value of 3.35 shows that the Freundlich isotherm is more suitable model for describing PCP adsorption on the MFC adsorbent. These results also suggest that PCP adsorption may occur on both the homogeneous and the heterogeneous surface sites of the MFC adsorbent [11]. Moreover, from the linearization fitting with the Langmuir model, the calculated  $q_{\max}$  value for PCP adsorption on the MFC sample was 122.25 mg/g. This value of  $q_{\max}$  is close to previous studies on carbon-based adsorbents [5] and significantly higher than those reported for materials such as eggshell powder, chitosan, corn waste, and others [12-14].

Subsequently, the durability and recyclability of MFC for PCP adsorption were evaluated. Fig. 6 presents the ADE of PCP on MFC materials over 5 adsorption recycles. The adsorbent dosage, PCP concentration, and pH of solution were adjusted to 300 mg/L, 10 mg/L, and 5.0, respectively. The data reveal a minimal decrease of 5.77% in the ADE values, from 96.53% initially to 90.76% after the 5th recycle. These results demonstrate that, MFC materials possess excellent durability and recyclability for the adsorptive removals of PCP in aqueous solution under the investigated conditions.

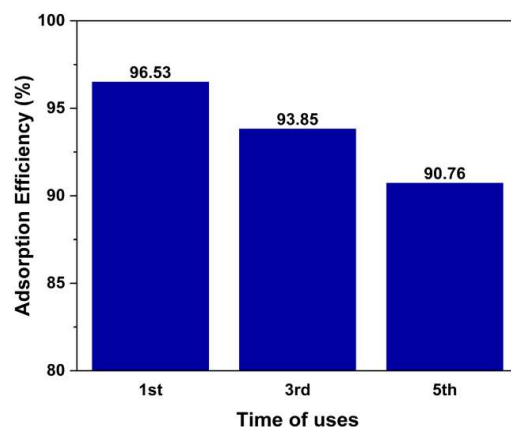


Figure 6. PCP adsorption efficiency for several uses

#### 4. CONCLUSION

In this study, the domestic ACs was successfully fabricated with magnetic MFO NPs by a simple and low-cost gel combustion method. Material characterization verified the formation of cubic-like spinel MFO NPs on AC sheet with high  $S_{\text{BET}}$  of 649.3  $\text{m}^2/\text{g}$  and a saturation magnetization value of 15.98 emu/g under an applied magnetic field of -10k to 10k Oe. The experimental series of PCP adsorption on MFC adsorbent showed a highest ADE of 96.53% for 10 mg/L PCP at pH 5 after 24 hours of adsorption with an MFC dosage of 300 mg/L. The study also indicated that PCP adsorption onto MFC was well-fitted by both Langmuir and Freundlich isotherm model, with the maximum adsorption capacity of 122.3 mg/g.



## REFERENCE

1. Rong Y., Han R., *Adsorption of p-chlorophenol and p-nitrophenol in single and binary systems from solution using magnetic activated carbon*, Korean J Chem. Eng., 2019, **36**:942-953. DOI:10.1007/s11814-019-0267-1
2. *Oluwasanu AA Fate and Toxicity of Chlorinated Phenols of Environmental Implications: A Review*, Med. Anal. Chem. Int. J., 2018, **2**(4):000126. DOI:10.23880/MACIJ-16000126
3. Polati S., Gosetti F., Gianotti V., Gennaro M., *Sorption and desorption behavior of chloroanilines and chlorophenols on montmorillonite and kaolinite*, J. Environ. Sci. Heal Part B Pestic Food Contam. Agric. Wastes, 2006, **41**:765-779. DOI:10.1080/03601230600805774
4. Yousef R. I., El-Eswed B., *Adsorption behavior of chlorophenols on natural zeolite*, Sep. Sci. Technol., 2007, **42**:3187-3197. DOI:10.1080/01496390701514873
5. Mollah A. H., Robinson C. W., *Pentachlorophenol adsorption and desorption characteristics of granular activated carbon - I. Isotherms*, Water Res., 1996, **30**:2901-2906. DOI:10.1016/S0043-1354(96)00131-5
6. Liu X., Tian J., Li Y., et al., *Enhanced dyes adsorption from wastewater via Fe<sub>3</sub>O<sub>4</sub> nanoparticles functionalized activated carbon*, J. Hazard Mater., 2019, **407**: 373-397. DOI:10.1016/j.jhazmat.2019.03.103
7. Jiang T., Liang Y., He Y., Wang Q., *Activated carbon/NiFe<sub>2</sub>O<sub>4</sub> magnetic composite: A magnetic adsorbent for the adsorption of methyl orange*, J. Environ. Chem. Eng., 2015, **3**:1740-1751. DOI:10.1016/j.jece.2015.06.020
8. Xu J., Xin P., Gao Y., et al., *Magnetic properties and methylene blue adsorptive performance of CoFe<sub>2</sub>O<sub>4</sub>/activated carbon nanocomposites*, Mater. Chem. Phys., 2014, **147**:915-919. DOI:10.1016/j.matchemphys.2014.06.037
9. Le H. B., Nghiem T. X., Nguyen K. T., et al., *Efficient photocatalytic remediation of persistent organic pollutants using magnetically recoverable spinel manganese ferrite nanoparticles supported on activated carbon*, Materials Research Bulletin, 2024, **178**:112913. DOI:10.1016/j.materresbull.2024.112913
10. González-López M. E., Laureano-Anzaldo C. M., Pérez-Fonseca A. A., et al., *A critical overview of adsorption models linearization: Methodological and statistical inconsistencies*, Sep. Purif. Rev., 2022, **51**:358-372. DOI:10.1080/15422119.2021.1951757
11. El Qada E. N., Allen S. J., Walker G. M., *Adsorption of Methylene Blue onto activated carbon produced from steam activated bituminous coal: A study of equilibrium adsorption isotherm*, Chem. Eng. J., 2006, **124**:103-110. DOI:10.1016/j.cej.2006.08.015
12. Shankar A., Kongot M., Saini V. K., Kumar A., *Removal of pentachlorophenol pesticide from aqueous solutions using modified chitosan*, Arab. J. Chem., 2020, **13**:1821-1830. DOI:10.1016/j.arabjc.2018.01.016

13. Kuśmierk K., Idzskiewicz P., Sświętkowski A., Dąbek L., *Adsorptive removal of pentachlorophenol from aqueous solutions using powdered eggshell*, Arch. Environ. Prot., 2017, **43**:10-16. DOI:10.1515/aep-2017-0029
14. Abdel-Ghani N. T., El-Chaghaby G. A., Zahran E. M., *Pentachlorophenol (PCP) adsorption from aqueous solution by activated carbons prepared from corn wastes*, Int. J. Environ. Sci. Technol., 2015, **12**:211-222. DOI:10.1007/s13762-013-0447-1

### SUMMARY

This work involved the synthesis of magnetized activated carbon (AC) incorporated with manganese ferrite (MFO) nanoparticles (NPs), denoted as MFC and the evaluation of its adsorptive removals of pentachlorophenol (PCP). A simple and low-cost gel combustion method was employed for the preparation. The material characterization confirmed the presence of cubic-like spinel MFO NPs on the ACs, with a size of 11.63 nm. The calculated specific surface area ( $S_{BET}$ ) obtained from  $N_2$  adsorption isotherm was  $649.3 \text{ m}^2/\text{g}$ , whereas the saturation magnetisation value was found to be  $15.98 \text{ emu/g}$  within an applied magnetic field ranging from  $-10\text{k}$  to  $10\text{k}$  Oe. The study on the adsorption of PCP on MFC absorbent demonstrates the highest adsorption efficiency (ADE) of 96.53% for an initial PCP concentration of  $10 \text{ mg/L}$  at pH 5 after 24 hours of adsorption using an MFC content of  $300 \text{ mg/L}$ . Ultimately, the adsorption of PCP on MFC conformed to both the Langmuir and Freundlich isotherm models, with a maximum adsorption capacity of  $122.25 \text{ mg/g}$ , indicating that PCP molecules were effectively adsorbed on both homogeneous and heterogeneous sites of the adsorbent.

**Keywords:** *Activated carbon, manganese ferrite, pentachlorophenol, adsorption, persistent organic pollutants.*

<sup>(1)</sup> *Joint Vietnam-Russia Tropical Science and Technology Research Center, 63 Nguyen Van Huyen, Cau Giay, Hanoi, Vietnam*

<sup>(2)</sup> *Institute of Materials Science, Vietnam Academy of Science and Technology, 18 Hoang Quoc Viet, Cau Giay, Hanoi, Vietnam*

<sup>(3)</sup> *Graduate School of Science and Technology, Vietnam Academy of Science and Technology, 18 Hoang Quoc Viet, Cau Giay, Hanoi, Vietnam*

*Nhận bài ngày 20 tháng 6 năm 2024*

*Phản biện xong ngày 30 tháng 6 năm 2024*

*Hoàn thiện ngày 05 tháng 7 năm 2024*

**Contact: Le Bao Hung**

Department of Chemistry and Environment, Joint Vietnam-Russia Tropical Science and Technology Research Center

63 Nguyen Van Huyen, Cau Giay, Hanoi, Vietnam

Tel: +84982201881; Email: baoleh@gmail.com